Reductive dechlorination of 2,3-dichloroaniline by *Dehalobacter* in an anaerobic enrichment culture

Shuping Wang,[1] Sofia P. Araújo,[2,3] Line Lomheim,[2] E. Erin Mack,[4] Elizabeth A. Edwards,[2*] and Elodie Passeport[1,2,5*]

[1]Department of Civil & Mineral Engineering, University of Toronto
35 St. George Street, Toronto, Ontario, M5S 1A4, Canada

[2]Department of Chemical Engineering & Applied Chemistry, University of Toronto
200 College Street, Toronto, Ontario, M5S 3E5, Canada

[3]Departamento de Engenharia Civil e Ambiental, Universidade Federal de Pernambuco, Recife, Pernambuco, 50740-530, Brazil

[4]Corteva Environmental Remediation, Corteva Agriscience, Wilmington, DE, 19805, USA

[5]Department of Environmental Sciences, Rutgers University, 14 College Farm Rd, New Brunswick NJ 08901, USA

*Corresponding authors: elodie.passeport@rutgers.edu, +1 848-932-6740
elizabeth.edwards@utoronto.ca, +1 416-946-3506

1 ABSTRACT

2,3-dichloroaniline (2,3-DCA) has widespread use in chemical manufacturing and remains a persistent groundwater contaminant. To better understand the pathway and kinetics of its reductive dechlorination, we conducted a laboratory kinetic experiment using an anaerobic enrichment culture dominated by *Dehalobacter*. At an initial field-relevant concentration of 40 mg/L, complete and stoichiometric dechlorination of 2,3-DCA to aniline via 2-CA was achieved. The intermediates, 2-chloroaniline (2-CA) and 3-chloroaniline, were transiently formed in a ratio of 8:1. The growth yields of *Dehalobacter* on 2,3-DCA and 2-CA were $1.2 \pm 0.1 \times 10^8$ and $1.3 \pm 0.1 \times 10^8$ 16S rRNA gene copies/μmol chloride, respectively. The maximum specific growth rate for 2,3-DCA, μ_{max}, was 0.18 ± 0.03 day^{-1} with a half-saturation constant, K_s, at 45 ± 16 mg /L. The first-order decay constant for *Dehalobacter* when starved of chlorinated electron acceptors was estimated at 0.017 ± 0.001 day^{-1}. Lactate fermentation, acetogenesis from ethanol, syntrophic propionate oxidation, and hydrogenotrophic methanogenesis were observed during dechlorination. This work provides insights into the organohalide respiration of 2,3-DCA to aniline and advances the understanding of microbial interactions during anaerobic dechlorination. These results offer guidance for developing stable dechlorinating microbial ecosystems and key kinetic parameters for predictive modeling of groundwater 2,3-DCA fate and transport.

2 Keywords

Biotransformation, Anaerobic microbial community, Organohalide respiration, Reductive dechlorination, Syntrophy, Microbial kinetics

3 Synopsis

This study demonstrated stoichiometric dechlorination of 2,3-dichloroaniline to aniline, characterized syntrophic interactions in a mixed anaerobic dechlorinating culture, and determined growth yield, first-order decay and Monod constants for *Dehalobacter*.

Graphical abstract

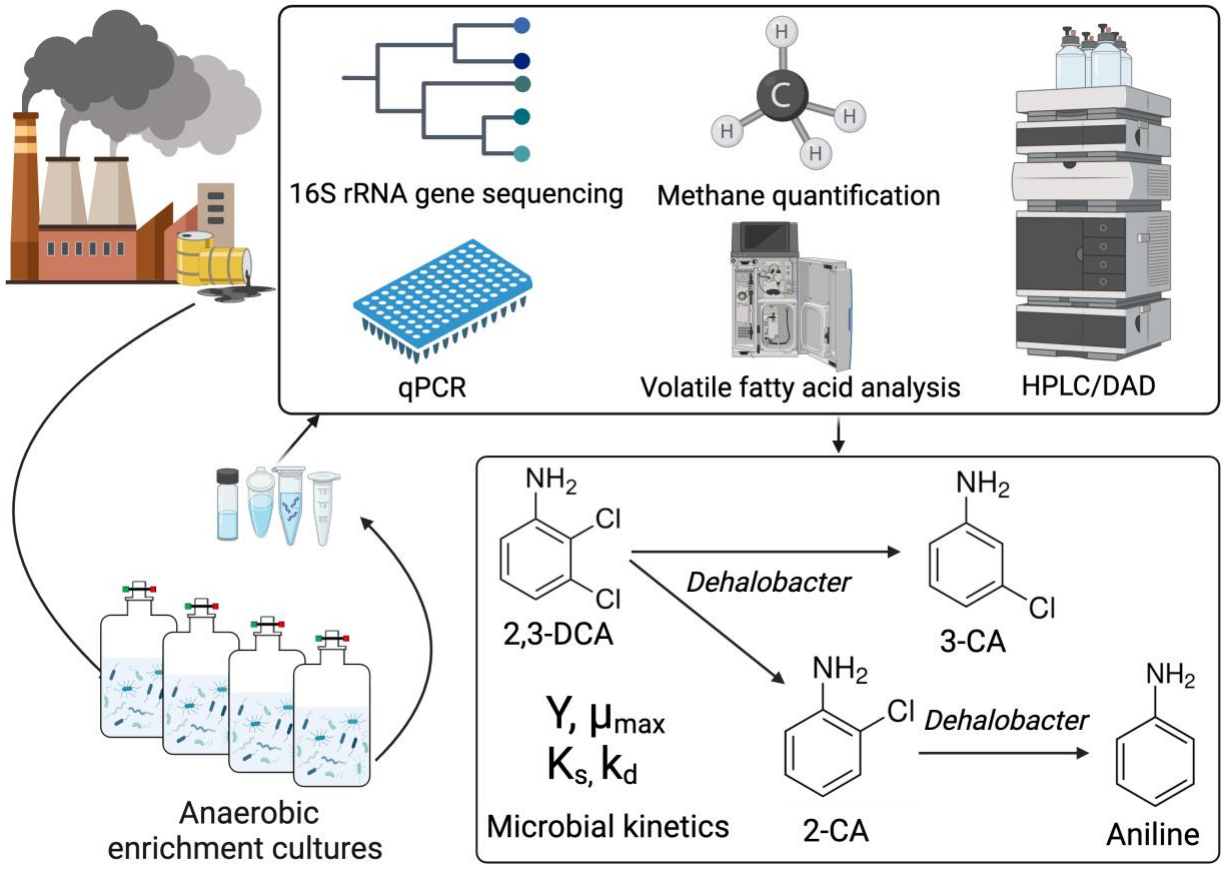

Created in BioRender. Wang, S. (2025) https://BioRender.com/f47t993

4 INTRODUCTION

Dichloroaniline (DCA) isomers are a class of amino-substituted chlorinated aromatic compounds that are widely used as intermediates in the manufacture of various chemical products, including herbicides, cosmetics, pigments, pharmaceuticals, and antimicrobials.[1] DCAs are primarily released into the environment through improper handling and disposal during industrial processes. They are also produced from natural attenuation of phenylurea herbicides and nitro-substituted aromatics.[2–4] Due to high chemical stability and toxicity, DCA contamination poses a significant environmental challenge, particularly in aquatic and soil ecosystems.[5–7]

Contaminated groundwater environments, which are often anoxic, provide favorable conditions for organohalide respiration. Such processes have proven successful for many halogenated pollutants, particularly chlorinated alkenes and alkanes.[8–12] However, studies on the reductive dechlorination of DCAs remain limited.

Reductive dechlorination of DCAs was first observed using pond sediment[13] and aquifer slurries[14]. The latter study reported the biotransformation of 3,4-DCA (around 50 μM) to 3-chloroaniline (3-CA) during the 8-month experiment.[14] Similarly, Susarla et al. (1998) observed reductive dechlorination of 3,4-DCA (4 μM) using sulfidogenic estuarine sediment with 3-CA and aniline as the end products.[15] However, these early studies used low DCA concentrations and often required extended incubation periods (e.g., >200 days) for complete transformation. Moreover, the microorganisms responsible for these anaerobic transformations were not identified and the relatively poor mass balance obtained in these studies limited the understanding of the underlying organohalide respiration pathways.

More recent studies have identified microorganisms capable of organohalide respiration using DCAs. Duc and Oanh (2019) isolated *Geobacter* sp. KT5 from contaminated river sediment,

78 which grew on a wide range of chlorinated anilines (50 μM) and transiently produced
79 dechlorinated metabolites such as 3-CA, aniline and 4-aminobenzoate.[16] Cooper et al. (2015)
80 showed that organohalide respiring *Dehalococcoides* strain CBDB1 could respire and
81 dechlorinate 2,3-DCA (but not 2,4- or 2,6-DCA) with H_2 as electron donor.[17] In a follow up
82 study contrasting dechlorinating mechanisms between *Dehalococcoides mccartyi* strain CBDB1
83 and *Dehalobacter* sp. strain 14DCB1 previously isolated on chlorinated benzenes, the authors
84 found that both strains could transform 2,3-DCA and 3,4-DCA with hydrogen as the electron
85 donor producing 3-CA (by CBDB1) or very minor amounts of 2-chloroaniline (2-CA, by
86 14DCB1) and 3-CA (by 14DCB1).[18] Despite these advances, no studies have focused on
87 achieving complete and stoichiometric anaerobic transformation of DCAs to aniline at
88 concentrations relevant to those observed at a highly contaminated site[19–21] with average total
89 DCA concentrations above 200 μM in groundwater. Furthermore, although *Dehalobacter* can
90 transform a variety of halogenated organic contaminants (e.g., chlorinated ethanes, toluene,
91 benzenes, and chloroform),[22–24] reproducible and robust microbial kinetics of *Dehalobacter*-
92 mediated dechlorination are lacking, limiting the predictability and quantification of natural or
93 bioaugmented dechlorination at contaminated sites. The interactions between *Dehalobacter* and
94 other microorganisms in dechlorinating microbial consortia also remain poorly understood. In a
95 companion study, subtle aniline formation was observed after 2,3-DCA dechlorination to 2-CA
96 in culture 23DCA-T2.[25] We made a transfer from this culture and the resulting subculture
97 surprisingly exhibited significantly more aniline formation. This prompted us to further explore
98 dechlorination of 2,3-DCA to aniline and *Dehalobacter* kinetics. The objectives of our study
99 were to: (1) demonstrate the complete reductive dechlorination of 2,3-DCA to aniline via 2-CA
100 at a high initial concentration; (2) identify the associated transformation pathway; (3) determine

growth yield and kinetic parameters to improve the predictability of dechlorination and (4) investigate syntrophic interactions between cocultured microorganisms and *Dehalobacter*. These objectives were achieved by frequent (every 3 days) sampling of chemical and microbial concentrations in stable enrichment cultures derived from a contaminated site.

5 MATERIALS AND METHODS

5.1 Chemicals

All chemicals were obtained from Sigma Aldrich (St. Louis, Missouri, USA) unless otherwise noted. Cultures were amended with 2,3-DCA (99.6% purity). Aniline and 2-CA used as standards were both at 99.5% purity; whereas, 3-CA and 4-chloroaniline (4-CA) were 99% and 98% pure, respectively. Ethanol was HPLC grade. Sodium lactate (60% by mass) was purchased from Spectrum Chemical MFG Corp.

5.2 Microbial Enrichment Cultures

The culture used as an inoculum in this study was the third consecutive subculture (referred to as WANG-23DCA-T3) from an anaerobic methanogenic 2,3-DCA-dechlorinating enrichment culture (i.e., 23DCA-T2), described in Araújo et al. (2025).[25] In brief, 23DCA-T2 originated from microcosms established in 2015 using groundwater and soil samples collected from a heavily contaminated industrial site in Brazil (Supporting Information (SI) Figure S1).[25] On May 4, 2022, the first transfer (WANG-23DCA-T1) was prepared by inoculating 90 mL of anaerobic medium with 10 mL 23DCA-T2 sample. After three-month cultivation, on August 9, 2022, a 50 mL portion of culture WANG-23DCA-T1 was transferred to establish a new subculture (WANG-23DCA-T2). On day 188 of WANG-23DCA-T2 (February 13, 2023), a 3% transfer of culture (12 mL) from WANG-23DCA-T2 was made to establish subculture WANG-23-DCA-T3

123 (400 mL). All three subcultures were repeatedly amended with 2,3-DCA and demonstrated
124 activity in transforming it, with WANG-23-DCA-T3 showing particularly strong conversion of
125 2,3-DCA to aniline. These subcultures were topped up with medium multiple times to build up
126 culture volume for future experiments. On day 254 of WANG-23-DCA-T3 (October 25, 2023),
127 the inoculum for this study was taken from WANG-23-DCA-T3. Dechlorination profiles and
128 associated cultivation conditions for subcultures and transfers are detailed in SI Section S1 and
129 Figures S2-S4.

130 5.3 Experimental Setup

131 In this study, all experiments were performed in an anaerobic glovebox (Vinyl Anaerobic
132 Chamber glovebox, Coy Laboratory Products) at room temperature (21-22°C). The glovebox
133 was filled with a gas mix of 10% H_2, 10% CO_2 and 80% N_2, however owing to reaction with
134 diffusing oxygen, the H_2 concentration in the glovebox remained around 1-1.5% H_2.
135 To establish the dechlorination kinetics, four replicates with an initial concentration of 40 mg/L
136 (i.e., 250 μM) 2,3-DCA and 3% (v/v) inoculum were prepared in autoclaved 250-mL Boston
137 round glass bottles sealed with Mininert valves, with an initial medium volume of 210 mL and
138 headspace volume of 40 mL. They are referred to as "biotic bottles". The medium used in this
139 study was a pre-reduced mineral medium described in Edwards and Grbic-Galić (1992).[26] To
140 estimate the decay kinetics of *Dehalobacter* under conditions lacking electron acceptors,
141 triplicate decay bottles were established in the same manner as the biotic bottles, excluding the
142 addition of 2,3-DCA. To monitor the mass loss due to sampling and control for the possibility of
143 abiotic transformation processes, triplicate abiotic controls were set up similarly without
144 inoculation in autoclaved 250-mL Boston round bottles, each containing 210 mL of mineral
145 medium spiked at 40 mg/L of 2,3-DCA. Biotic and abiotic bottles were amended with 2,3-DCA

146 by dropping a feeding vial containing 2,3-DCA into the bottle. Details are provided in Section
147 S2. After spiking with 2,3-DCA, the concentration of 2,3-DCA was regularly monitored in all
148 bottles. Inoculation of the biotic bottles was not conducted until the concentration of 2,3-DCA
149 had stabilized at the target concentration (i.e., 40 mg/L), which took three days. Once complete
150 dissolution of 2,3-DCA was attained, 6.5 mL of homogenized, active inoculum was added to
151 four biotic bottles. The biotic and decay bottles were then amended with sodium lactate (0.6
152 mM) and ethanol (3.3 mM). Abiotic controls did not receive any amendment of electron donors.
153 The inoculation defined the time zero of the experiment. Samples were collected immediately
154 after inoculation to characterize the initial concentration of methane (headspace), 2,3-DCA,
155 transformation products, volatile fatty acids, inorganic anions, *Dehalobacter* abundance, and
156 microbial community composition. During the experiment, all the bottles were covered with
157 black cloth to minimize exposure to light and possible photodegradation.
158 Aqueous samples (350 μL) were taken from biotic and abiotic bottles approximately three times
159 every week for chloroaniline and aniline analysis. A 4-mL sample was collected for DNA
160 extraction from biotic and decay bottles roughly every ten days. Samples (500 μL) for
161 quantifying inorganic anions and volatile fatty acids were taken weekly from biotic and abiotic
162 bottles. Headspace samples (300 μL) for determining methane production were withdrawn
163 approximately once every ten days from the biotic bottles. The total liquid volume withdrawn
164 did not exceed 20% of the initial volume during the first 50 days (i.e., dechlorination of 2,3-DCA
165 to 2-CA and 3-CA). Sample collection and processing are detailed in the SI.

166 5.4 Analytical procedures

167 Chloroanilines and aniline were measured using high-performance liquid chromatography
168 coupled with a diode array detector (HPLC/DAD, Thermo Scientific Dionex Ultimate 3000

169 series) equipped with an Accucore C18 column (100 mm × 2.1 mm × 2.6 µm) and guard column
170 (10 mm × 2.1 mm × 2.6 µm; Thermo Scientific, Waltham, MA, USA). Methane and other
171 possible volatiles (e.g., benzene) were measured by a Hewlett-Packard 5890 Series II gas
172 chromatograph (GC) using a GSQ I. D. PLOT column (30 m × 0.53 mm; J & W Scientific,
173 Folsom, USA) configured with a flame ionization detector (FID). Inorganic anions (sulfate,
174 phosphate, nitrate, nitrite, and chloride) and volatile fatty acids (VFAs; acetate, propionate,
175 butyrate, lactate, formate, and pyruvate) were measured by ion chromatography (IC) using a
176 Dionex™ Integrion™ high pressure IC coupled with an ASRS 500 suppressor and a Dionex™
177 AS-DV autosampler (Thermo Fisher Scientific). Separation was achieved using a Dionex™
178 IonPac™ 2 × 250 mm AS11-HC column. Analytical methods are detailed in Sections S3-S5. The
179 limits of quantification (LOQs) were 0.7 µmol/L for 2,3-DCA, 0.8 µmol/L for 2-CA and 3-CA,
180 1.5 µmol/L for aniline, 0.003 mmol/L for lactate, and 0.001 mmol/L for all other target VFAs
181 (Section S5).

182 5.5 DNA sampling and extraction

183 Culture samples (4 mL) were withdrawn for DNA extraction and centrifuged (described in
184 Section S6), supernatant discarded, and the cell pellets were stored at -80 °C. DNA was extracted
185 using the DNeasy PowerSoil Pro kit (Qiagen) following manufacturer's guidelines. DNA was
186 eluted in 50 µL of 10 mM Tris-HCl buffer and stored at -80 °C until analysis.

187 5.6 Quantitative PCR analysis

188 Quantitative polymerase chain reaction (qPCR) primer sets targeting *Dehalobacter* (Dhb) were
189 used as previously described.[27] Primer sequences were Dhb477f (5'-
190 GATTGACGGTACCTAACGAGG-3') and Dhb647r (5'-TACAGTTTCCAATGCTTTACG-

191 3').[27] Primers targeting most bacteria (Bac) were as follows: Bac1055f (5'-
192 ATGGCTGTCGTCAGCT-3') and Bac1392r (5'-ACGGGCGGTGTGTAC-3').[28] Temperature
193 profiles and reaction details are available in Section S7. The qPCR results with *Dehalobacter*
194 biomass estimation are provided in Table S1.

195 5.7 16S rRNA gene amplicon sequencing

196 16S rRNA gene amplicon sequencing targeting the V6-V8 region of bacteria and archaea was
197 carried out using the Illumina NovaSeq PE300 platform at Genome Québec (Montreal, QC,
198 Canada), using a set of modified "staggered end" primers: forward primer 926f (5'-
199 AAACTYAAAKGAATWGRCGG-3') and reverse primer 1392r (5'-ACGGGCGGTGWGTRC-
200 3', as previously described.[29] Original amplicon reads were processed using QIIME 2 (v.2021.2)
201 (Section S8).[30] Amplicon sequence variants (ASVs) were generated using DADA2 plugin [31] and
202 taxonomically classified with the SSU SILVA v.138 database.[32] Relative abundance of ASVs in
203 bacterial (Table S2) and archaeal (Table S3) communities were calculated. Sequence alignment
204 for *Dehalobacter* ASVs was performed in Geneious Prime (v.2023.1.2) using the MUSCLE
205 Alignment feature. Original sequence reads are available through NCBI (Accession:
206 PRJNA1040917).

207 5.8 Modeling dechlorination of 2,3-DCA using Monod kinetics

208 We applied the Monod equations[33,34] to estimate the kinetic parameters for *Dehalobacter* growth
209 on 2,3-DCA with two coupled non-linear differential equations that describe the growth of
210 *Dehalobacter* (Eq. 1) and the associated consumption of the limiting substrate (Eq. 2):

211 $$\frac{dX}{dt} = \mu_{max} X \left(\frac{S}{S + K_s}\right) - k_d X$$

212 *Equation (1)*

213 $$-\frac{dS}{dt} = \frac{\mu_{max}X}{Y}\left(\frac{S}{S+K_s}\right)$$

214 *Equation (2)*

215 where S and X represent concentrations (g/L) of the substrate (2,3-DCA or 2-CA) and active
216 biomass (*Dehalobacter*) at time t, respectively; Ks is the half-saturation constant (g/L), and μ_{max}
217 is the maximum specific growth rate (day^{-1}); Y is the growth yield (g biomass /g substrate); k_d is
218 the first-order decay constant (day^{-1}) for biomass; dX/dt is the growth rate of biomass (g/L/day),
219 and -dS/dt is the substrate consumption rate (g/L/day).

220 Yield and decay parameters Y and k_d were independently determined in this study. Therefore, K_s
221 and μ_{max} were the only two Monod parameters obtained through the least squares optimization.
222 The time-course substrate depletion data were used to fit the Monod model. The coupled
223 differential equations were numerically solved using the "solve_ivp" function from the
224 "scipy.integrate" module in Python, with initial conditions set to the substrate and biomass
225 concentrations measured at time zero (S_0 and X_0, respectively). S_0 was well constrained, but X_0
226 being a less accurate measurement was allowed to vary within a narrow range during
227 optimization. The optimal initial biomass for modelling is referred to as X_0'. The combined
228 residual sum of squares (RSS) from all replicates was minimized. We employed the
229 "least_squares" function from the "scipy.optimize" module in Python to achieve the best fit by
230 adjusting optimization parameters, K_s, μ_{max}, and X_0' for 2,3-DCA dechlorination. The starting
231 biomass used for modeling the subsequent 2-CA dechlorination was calculated from the kinetics
232 of the preceding 2,3-DCA dechlorination step. Thus, for 2-CA dechlorination kinetics, only K_s
233 and μ_{max} were adjusted to minimize RSS. To accommodate the determination of K_s and μ_{max},
234 broad parameter ranges were applied ([0,1000] mg/L for K_s and [0,10] $day^{-1}$for μ_{max}). A range of
235 [X_0/2, 4X_0] for X_0' was set to account for potential estimation errors associated with the initial

236 biomass measurement using qPCR. The goodness-of-fit was assessed using RSS, reduced chi-
237 square, and root-mean-square errors (RMSE).

238 6 RESULTS AND DISCUSSION

239 6.1 Complete dechlorination of 2,3-DCA to aniline via 2-CA

240 We observed complete and stoichiometric transformation of 2,3-DCA to aniline via 2-CA in all
241 four biotic replicates. The data for Biotic Bottle I is shown in Figure 1a, with the results for the
242 other replicates available in Figure S5. In the abiotic controls, 2,3-DCA concentration remained
243 constant throughout the course of the experiment (Figure 1a) and no transformation products
244 were detected.
245 In the biotic bottles, between days 0 and 53, 2,3-DCA underwent quantitative dechlorination
246 without a significant lag phase (< 2 days), resulting in the formation of 2-CA and 3-CA at an
247 overall molar stoichiometric ratio of 7.6 (± 1.9): 1 (n=88 using all time points). Our observations
248 indicate that *Dehalobacter* preferentially removes the chlorine substituent at the meta position
249 relative to the amino group to produce 2-CA. This finding aligns with a previous study showing
250 the dechlorination of 2,3-DCA to 2-CA by *Dehalobacter* Strain 14DCB1.[18] However, in that
251 study, the formation of 2-CA was minimal (<0.8 μM) over five successive 2,3-DCA feeding
252 cycles at 40 μM across 35 days.[18] In contrast, we observed a 1:1 stoichiometric conversion of
253 2,3-DCA to CAs (mainly 2-CA). A mole balance analysis for each biotic replicate showed that
254 92 (± 4) % (n=4) of the reduction in 2,3-DCA can be explained by the production of
255 dechlorination intermediates 2-CA and 3-CA over the course of 50 days.
256 After day 50, 2-CA was further dechlorinated to aniline, whereas 3-CA persisted (Figures 1a and
257 S5). End products of this two-step dechlorination were predominantly aniline (89%), with 3-CA

258 constituting the balance. On day 103, complete dechlorination of 2-CA to aniline was observed.
259 Dechlorination of 2-CA was also quantitative as 88 (± 6) % (n=3) of 2-CA consumed can be
260 attributed to the corresponding increase in the aniline concentration. Dechlorination of 2,3-DCA
261 to aniline is a sequential process. Dechlorination of 2-CA to aniline did not start until 2,3-DCA
262 was depleted in the bottles. This observation aligns with the results from the parent culture
263 (Figure S4), which shows that aniline formation began when 2-CA concentration was much
264 higher than 2,3-DCA concentration.
265 The preferential utilization of 2,3-DCA as an electron acceptor by *Dehalobacter* over 2-CA is
266 consistent with the reported Gibbs free energy under standard conditions for dechlorination of
267 2,3-DCA to either 2-CA (-135.0 kJ/reaction) or 3-CA (-137.7 kJ/reaction), which are more
268 thermodynamically favorable than the dechlorination of 2-CA to aniline (-126.8 kJ/reaction).[35]
269 Moreover, this preferential utilization may explain the negligible aniline formation in the earlier
270 subcultures (Figures S2 and S3), where 2,3-DCA was re-amended before its depletion and
271 consistently available to *Dehalobacter*.

272 6.2 *Dehalobacter* is responsible for dechlorination

273 A continuous and consistent rise in *Dehalobacter* absolute abundance (16S rRNA gene copies/L)
274 was observed across all biotic replicates during both the 2,3-DCA and 2-CA dechlorination
275 stages (Figure 1c). Biotic bottle II showed lower *Dehalobacter* growth during 2-CA
276 dechlorination compared to other replicates, but this aligns with the limited dechlorination of 2-
277 CA to aniline in this bottle (Figure S5II), confirming the correlation between 2-CA
278 dechlorination and *Dehalobacter* growth. The results also indicate that *Dehalobacter* can be
279 enriched through the supply of 2,3-DCA and 2-CA (Figure 1.e). From days 12 to 87, the relative
280 abundance of *Dehalobacter* in the bacterial community increased by 46.9 ± 8.4% (n=4),

281 becoming the most dominant bacterial genus. In line with stoichiometry, the results demonstrate
282 that *Dehalobacter* can grow on 2,3-DCA and 2-CA through reductive dechlorination. Two
283 predominant ASVs (ASV3 and ASV4) accounted for 99.9 ± 0.1% (n=32) of total *Dehalobacter*
284 reads (Table S2). *Dehalobacter* ASV3 and ASV4 shared >99.78% 16S rRNA gene sequence
285 identity (differing by one base pair in the 468-bp amplicon) and exhibited consistent abundance
286 trends throughout the experiment, maintaining a stable ASV3/ASV4 ratio of 3.1 ± 0.1:1 (n=32)
287 in all the samples. Therefore, the two ASVs likely belong to the same *Dehalobacter* strain.
288 *Dehalobacter* ASV3 and ASV4 were not the dominant *Dehalobacter* ASVs (ASV1 and ASV2)
289 in the original parent culture (23DCA-T2)[25] but the ASVs were present in other enrichment
290 cultures stemming from the original site material. With approximately 97% sequence identity
291 (Table S4), both ASV3 and ASV4 are genetically distinct from the dominant ASV1 and ASV2
292 found in 23DCA-T2,[25] where slow and low-level aniline formation was noticed. While these
293 genetic differences may account for the distinct capability of using 2-CA as an electron acceptor
294 to yield aniline, future research should investigate this further.
295

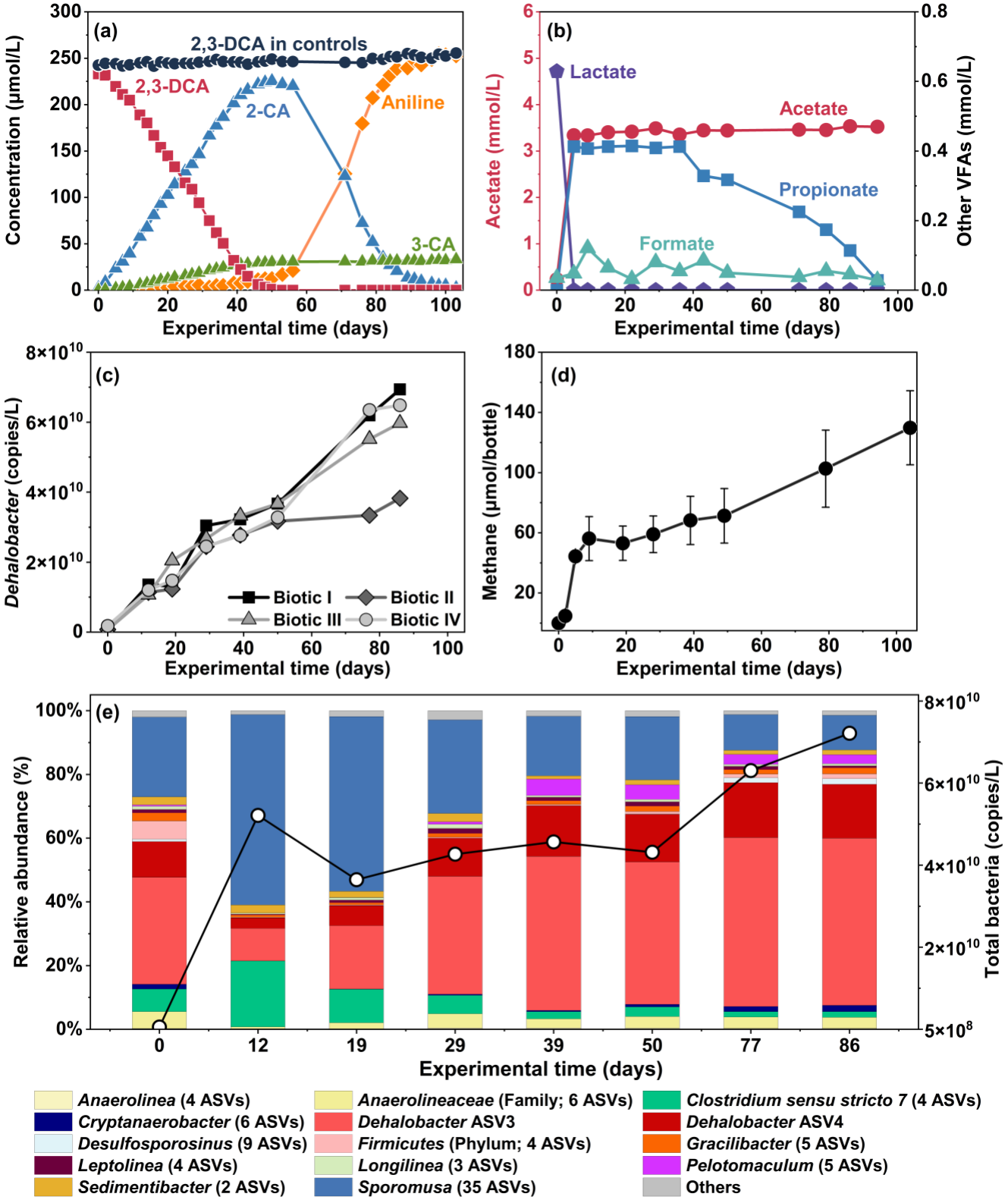

Figure 1. (a) Dechlorination of 2,3-DCA to aniline via 2-CA in biotic replicate I. Concentrations (μmol/L) of 2,3-dichloroaniline (2,3-DCA, red squares), 2-chloroaniline (2-

299 **CA, blue triangles), 3-chloroaniline (3-CA, green triangles), and aniline (orange diamonds)**
300 **over the experimental time (days) (Table S5). 4-CAwas not detected. Aniline and 3-CA are**
301 **shown as net formation by subtracting their initial concentrations. The average 2,3-DCA**
302 **concentrations of triplicate abiotic controls are represented by black circles. (b)**
303 **Concentration (mmol/L) of lactate (purple pentagons), acetate (red circles), propionate**
304 **(blue squares), and formate (light teal triangles) in replicate I. Butyrate and pyruvate were**
305 **not detected and fatty acid concentrations in abiotic controls remained below the LOQ**
306 **(Table S6). (c) Increase in *Dehalobacter* absolute abundance (16S rRNA gene copies/L) in**
307 **all biotic replicates. The absolute abundance was measured using qPCR with primers**
308 **targeting *Dehalobacter*. (d) Average methane production (µmol per bottle) of all biotic**
309 **replicates. Error bars represent the standard deviation among the four biotic replicates**
310 **(Table S7). (e) Changes in bacterial composition during dechlorination in replicate I. The**
311 **relative abundance of bacteria at the genus level (unless otherwise specified) obtained from**
312 **16S rRNA amplicon sequencing, shown as stacked bars, is presented in combination with**
313 **total bacterial concentrations (gene copies/L, shown on the secondary y-axis) determined**
314 **using qPCR targeting general bacteria. Others: ASVs with relative abundance < 1%.**
315 **Results from all four biotic replicates are provided in Figures S5, S6, S7a, and S7b.**
316

317

318 ## 6.3 Growth yields and microbial kinetics of *Dehalobacter*

319 ### 6.3.1 Growth yields and first-order decay

320 Through the two-step dechlorination process, we measured *Dehalobacter* growth yields on 2,3-
321 DCA and 2-CA (Figure 2). The growth yield for 2,3-DCA dechlorination was $1.2 \pm 0.1 \times 10^8$
322 16S rRNA gene copies/μmol 2,3-DCA converted (Figure 2a). Following the depletion of 2,3-
323 DCA, *Dehalobacter* continued to grow on 2-CA, with a growth yield of $1.3 \pm 0.1 \times 10^8$ 16S
324 rRNA gene copies/μmol 2-CA converted (Figure 2b). An extensive review of *Dehalobacter*
325 growth yields measured from various chlorinated organic compounds was conducted
326 previously.[25] For an easier comparison with other reported values, measured yields from this
327 study are converted into the same units (Table S8). Measured yields from this study are within
328 the range reported previously for 2,3-DCA and 3,4-DCA,[25] and are close to those previously
329 reported in the literature for other substrates including chlorinated ethanes and benzenes,[25]
330 falling on the higher end within one order of magnitude. Many studies underestimate the true
331 yield because the impact of cell decay is not considered. This impact becomes more significant
332 when data are analyzed over long-term cultivation (e.g., hundreds of days) and with a limited
333 number of samples. In this study, measurements of cell abundance were frequent and rates were
334 generally faster than many published studies, improving the estimate of yield. Moreover, this
335 study is the first to demonstrate the decay of *Dehalobacter* under stress conditions in the absence
336 of chlorinated organic compounds. After 62 days of starvation, the *Dehalobacter* concentration
337 in the triplicate decay bottles decreased to 35% of its initial level (Figure 2c). The first-order
338 decay constant was calculated as 0.017 ± 0.001 (n=3) day^{-1}, corresponding to a half-life of 41
339 days for *Dehalobacter* without chlorinated electron acceptors. Our results suggest that the
340 common assumption of zero decay in Monod kinetics may not be appropriate for modeling

341 *Dehalobacter* dynamics. Since the decay constant was measured under ample donor conditions,
342 donor limitation in the field could lead to even higher decay rates.
343 We converted the measured yield into mass units (g/g) assuming a mass per cell and 4 16S rRNA
344 gene copies per cell, yielding $1.7 \pm 0.2 \times 10^{-2}$ g *Dehalobacter*/ g 2,3-DCA and $2.4 \pm 0.2 \times 10^{-2}$ g
345 *Dehalobacter*/ g 2-CA. The theoretical maximum growth yields were also calculated applying
346 the McCarty TEEM model based on microbial energetics,[36,37] assuming hydrogen as the sole
347 electron donor, ammonium as the sole nitrogen source, and acetate as the sole carbon source
348 (Section S9). The predicted yields at various energy transfer efficiencies, along with the
349 measured yields are compared in Table S9. The thermodynamically predicted yields of
350 *Dehalobacter*, matched the experimental measurements when the energy transfer efficiency was
351 between 45% and 50% (Table S9). The consistency between predicted and measured values
352 gives confidence in the accuracy of the measured yields. The energy transfer efficiency range (45
353 – 50%) for *Dehalobacter* used in this study are consistent with the reported range (45 – 65%) for
354 anaerobic heterotrophic growth.[37]

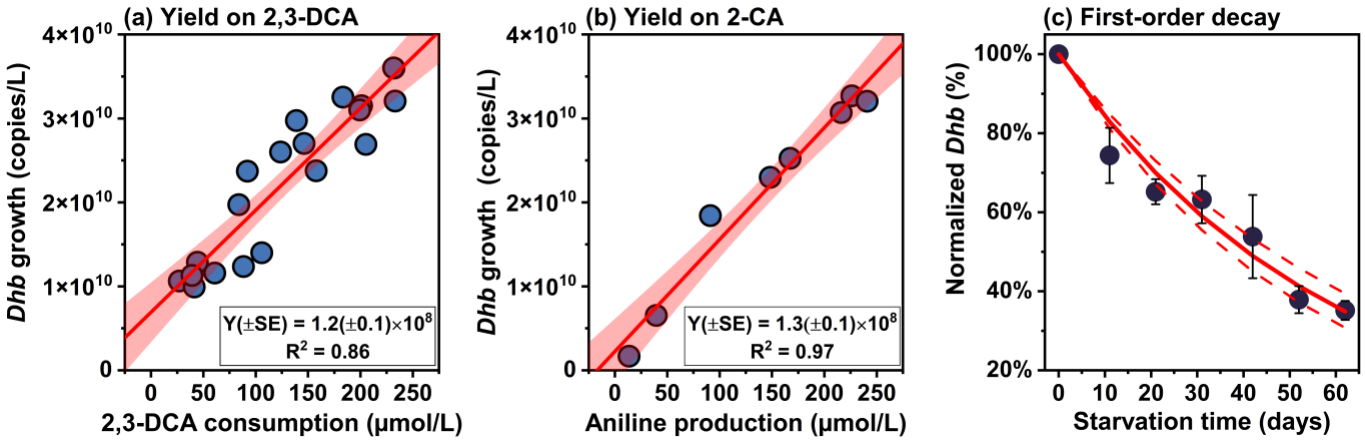

355
356
357 **Figure 2. Growth yields (panels a and b) and decay constant (panel c) for *Dehalobacter***
358 **(*Dhb*). Growth yields (Y) growing on 2,3-DCA and 2-CA are determined using Ordinary**
359 **Least Squares regression. Linear regressions are evaluated in Table S10. In panels a and b,**

solid red lines represent the fitted linear regression, with shaded areas corresponding to the 95% confidence interval. *Dhb* growth denotes the total increase in qPCR-determined *Dehalobacter* absolute abundance at each sampling time relative to the initial abundance at the start of each dechlorination stage. 2,3-DCA consumption represents the cumulative substrate (2,3-DCA) consumption at time t during 2,3-DCA dechlorination, while aniline production indicates the cumulative product (aniline) formation at time t during 2-CA dechlorination. As 2-CA was stoichiometrically converted to aniline, the growth yield on 2-CA was reported in gene copies per µmol 2-CA converted. SE: standard errors associated with the slope. The red line in panel c is the fitted first-order decay model, with dashed lines representing the 95 % confidence interval. Error bars represent the standard deviation in *Dehalobacter* levels normalized to the initial concentration (i.e., C_t/C_0) across decay bottles.

6.3.2 Modeling Monod kinetics to estimate K_s and μ_{max}

With the experimentally determined growth yields and decay constant, kinetics of dechlorination of chloroanilines can be modelled to determine K_s and μ_{max} using the Monod equation, assuming electron donor is not limiting. Optimal Monod constants and model evaluation are presented in Table S11. In the case of *Dehalobacter* growth on 2,3-DCA, K_s and μ_{max} are determined as 45 ± 16 mg/L and 0.18 ± 0.03 day^{-1}, respectively. Due to ample initial electron donor amendment (10-fold the demand for dechlorination of 2,3-DCA to aniline), electron donor limitation unlikely occurred during 2,3-DCA dechlorination. Reproducible trends of 2,3-DCA dechlorination were observed across all four replicates, and the minor variations between replicates can be explained by slight differences (±25%) in the initial biomass (Figure 2). The optimal μ_{max} results in a doubling time for *Dehalobacter* growing on 2,3-DCA without donor limitation ranging from 3.3 to 4.6 days. This range aligns with the doubling time estimated using measured *Dehalobacter* abundance in the initial stage (days 0 to 12), which was 3.3 days. For 2-CA dechlorination, similar constants (K_s = 35 ± 24 mg/L and μ_{max} = 0.14 ± 0.06 day^{-1}) were found using data from

387 bottles I and IV, exhibiting complete dechlorination. Comparable Monod constants were found
388 for two dechlorination steps. The apparent K_s values estimated from the Monod fits are high,
389 likely reflecting not only the intrinsic substrate affinity of *Dehalobacter* but also microbial
390 interactions and possible nutrient limitations within this field-relevant consortium, which can
391 inflate K_s. Using μ_{max} and the measured K_d, we estimated the minimum substrate concentration
392 required to support net growth to be approximately 5 mg/L for 2,3-DCA or 2-CA. These values
393 offer more realistic benchmarks for bioaugmentation, though they may vary under different field
394 conditions due to potential changes in K_d. The μ_{max} of *Dehalobacter* during 2-CA dechlorination
395 was slightly lower than during 2,3-DCA dechlorination, aligning with the thermodynamic
396 predictions that each mole of 2,3-DCA dechlorinated can yield 11% more energy for
397 *Dehalobacter* growth compared to 2-CA, assuming identical energy transfer efficiencies (Table
398 S9). However, kinetics of 2-CA dechlorination varied among individual replicates. Biotic bottles
399 II and III showed that 2-CA dechlorination had slower kinetics, which may indicate that electron
400 donor-limiting conditions were reached during 2-CA dechlorination, as no additional donor was
401 added after T=0.

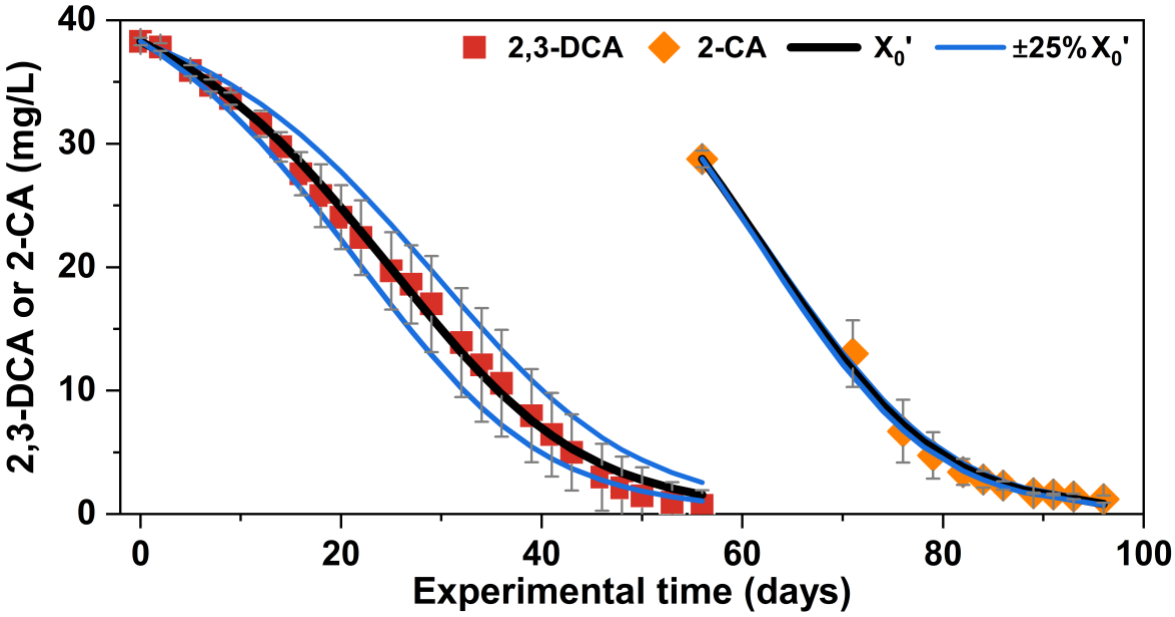

402

403 **Figure 3. Monod kinetics of dechlorination of 2,3-DCA to aniline. Three simulations were**
404 **performed at different initial biomass of *Dehalobacter* (75% X_0', 100% X_0', and 125% X_0'),**
405 **using the measured yields and decay constant, along with the optimal values for K_s and**
406 **μ_{max}. Red squares and orange diamonds represent the observed depletion data of 2,3-DCA**
407 **(from all four biotic replicates) and 2-CA (from biotic replicates I and IV), respectively,**
408 **with error bars showing the standard deviation across the replicates.**
409

6.4 Roles of other microbes in the consortium

Electron distribution and balances combining results from analyses of chloroanilines, fatty acids, and methane production were investigated to elucidate electron flows and syntrophic relationships within the anaerobic dechlorinating microbial consortium (Figures 4 and S8). This analysis is summarized in Section S10. Other than for biotic replicate IV that exhibited strangely slow acetogenesis, a good electron balance was achieved across replicates, at 84 ± 17 % (Table S12).

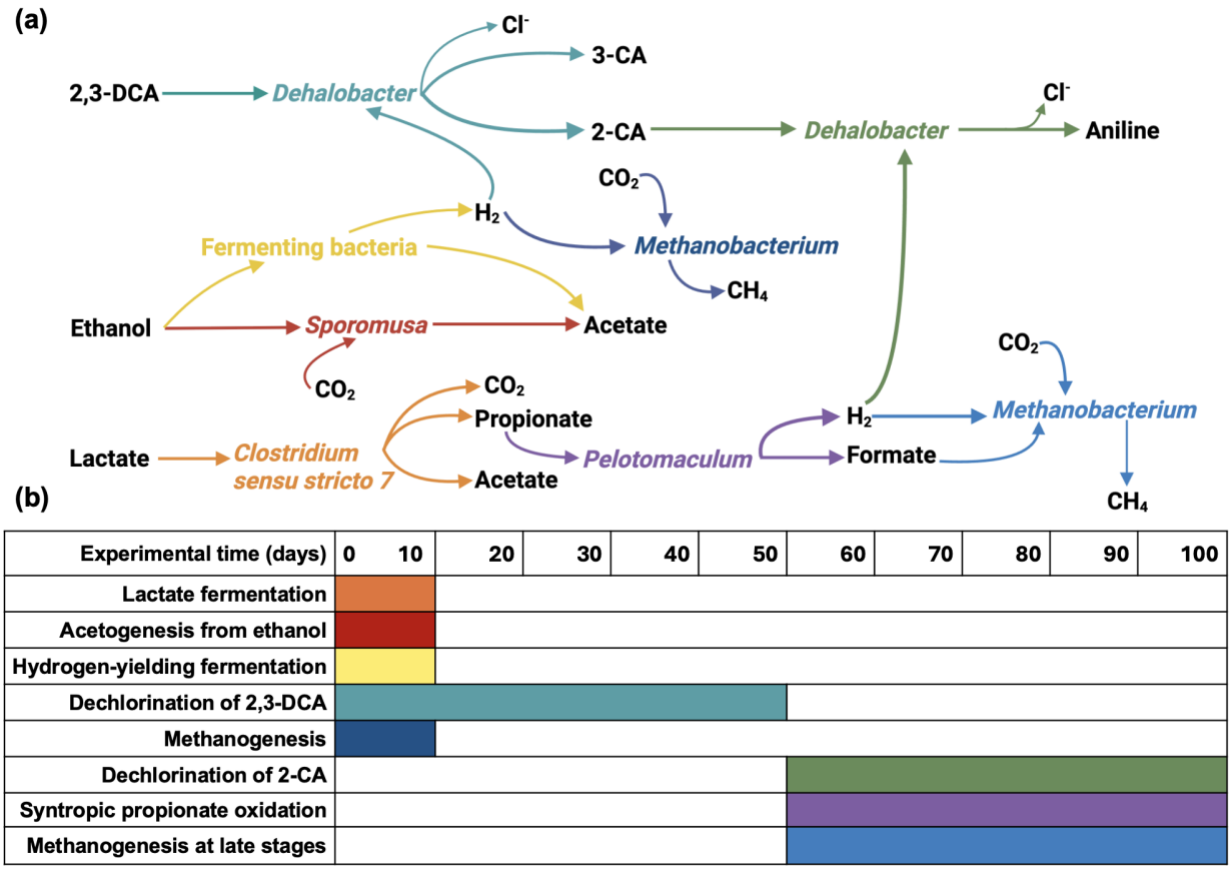

Created in BioRender. Wang, S. (2025) https://BioRender.com/rxovbel

Figure 4. Syntrophic relationships among representative microorganisms in the anaerobic dechlorinating microbial consortium (panel a) and temporal dynamics of major microbiological processes during the experiment (panel b). Electrons available for the whole system originated from the ethanol and lactate. Fermenting bacteria, possibly

423 ***Clostridium sensu stricto 7*, *Sporomusa*, and *Sedimentibacter*, consumed ethanol, releasing**
424 **electrons in the form of hydrogen gas (yellow; the hydrogen-yielding fermentation shown**
425 **refers to ethanol-based processes), which supported both 2,3-DCA dechlorination (teal) and**
426 **hydrogenotrophic methanogenesis (navy blue). However, a fraction of ethanol was**
427 **converted to acetate by *Sporomusa* (red) rather than to hydrogen. In contrast, lactate was**
428 **not initially used for hydrogen formation; instead, *Clostridium sensu stricto 7* converted**
429 **most of the amended lactate into acetate and propionate (orange). Subsequently,**
430 ***Pelotomaculum* oxidized propionate to release hydrogen (purple), supporting 2-CA**
431 **dechlorination (green) and the late-stage hydrogenotrophic methanogenesis (blue).**
432

433 6.4.1 Lactate fermentation and acetogenesis from ethanol to produce
434 acetate and hydrogen for *Dehalobacter*

435 We observed significant changes in the concentrations of volatile fatty acids between days 0 and
436 5 (Figures 1b and S6), especially production of acetate and propionate from added donors,
437 ethanol and lactate, indicating active fermentative processes early in the experiment. This finding
438 was also supported by 16S rRNA amplicon sequencing and total bacterial concentration data,
439 which revealed a notable growth of all fermenting bacteria, primarily *Clostridium sensu stricto 7*
440 and *Sporomusa*, dominating the bacterial community in the initial stage of the process (Figure 1e
441 and S7a). Additionally, methane production was observed during the same period (between day
442 0 and day 10, Figure 1d), indicating that methanogenesis aligned with fermentation. Microbial
443 data suggests that fermentative processes were hydrogen-yielding, as the dominant methanogenic
444 genus, *Methanobacterium*, is hydrogenotrophic (Figure S9).
445 Between days 0 and 5, lactate concentration, initially at 0.6 mM, decreased below the LOQ while
446 acetate, propionate, and formate concentrations increased (Figure 1e). Ethanol initially at 3.3
447 mM was presumably (the IC used to quantify the VFAs does not detect ethanol) also depleted in
448 the first 5 days because the electron balance is preserved (Figure S8). The stoichiometry ratio of

449 lactate consumed to propionate formed was 2.9 ± 0.2 : 2 (n=4; Section S11) for biotic replicates.
450 This ratio is consistent with the theoretical stoichiometry ratio of lactate: propionate: acetate = 3:
451 2: 1 during lactate fermentation to propionate and acetate (Section S11).[38,39] Therefore, this
452 observed ratio confirms that most of the lactate was fermented to propionate and acetate, and that
453 propionate was solely associated with lactate fermentation. The identified *Clostridium sensu*
454 *stricto 7* was likely responsible for lactate fermentation since species of *Clostridium* were
455 reported to convert lactate to propionate in a ratio of 3:2.[43,44]
456 Fermentative bacteria can alter their metabolic pathways to produce hydrogen in response to a
457 hydrogen demand.[42] *Clostridium sensu stricto* has also been documented to produce hydrogen
458 via fermentation.[43–45] Therefore, *Clostridium sensu stricto 7* along with other identified
459 fermenters, such as *Sedimentibacter* and *Sporomusa*, might be involved in hydrogen-yielding
460 fermentation from ethanol and fatty acids. Partnering with hydrogen consumers such as
461 *Dehalobacter* and methanogens, fermenting bacteria were able to oxidize ethanol to acetate,
462 presumably with hydrogen gas as a product.[46–48] The electron balance results indicate that the
463 electron demand for complete dechlorination is negligibly low compared to the electrons
464 supplied by ethanol (Figure S8b). Consequently, the hydrogen demand of *Dehalobacter* can be
465 readily met through hydrogen-yielding fermentation of ethanol.
466 The ratio of initial ethanol addition to measured acetate production, excluding acetate
467 contribution from lactate fermentation, was calculated as 1.2 ± 0.4 (n=4). This stoichiometry is
468 close to fermentation of ethanol to acetate and hydrogen (ethanol: acetate = 1:1)[42] and
469 acetogenesis from ethanol via the Wood-Ljungdahl pathway (ethanol: acetate = 1:1.5)[49].
470 Fermentation reactions are detailed in Section S11. The stoichiometry indicates hydrogen
471 production, and measured products suggest the coexistence of hydrogen-, formate- and non-

472 hydrogen-yielding acetogenesis during fermentation. Acetogenesis was mediated by *Sporomusa*,
473 as indicated by a significant increase in their abundance (Figure 1e). *Sporomusa*, a known
474 homoacetogen, can consume ethanol and CO_2 to produce acetate through the Wood-Ljungdahl
475 pathway[49]. Furthermore, the electron balance results suggested that only small fraction of
476 electrons from ethanol was used for hydrogen production, as the majority was converted into
477 acetate (Figure S8b).
478 The acetate pattern in biotic bottle IV differed noticeably from the other replicates, with a slow
479 increase in acetate over the course of the experiment, whereas the other replicates showed an
480 increase mainly within the first 10 days (Figures S6 and S8). This discrepancy on acetate
481 production suggests that biotic bottle IV received an erroneously small amount of ethanol at time
482 zero, potentially due to errors associated with syringe addition. Surprisingly, this discrepancy
483 allows us to identify *Sporomusa* as the primary acetate producer. The limited acetogenesis from
484 ethanol in biotic bottle IV significantly impacted its bacterial composition. In biotic bottle IV,
485 *Sporomusa* was much less abundant in the early stages of the experiment compared to the other
486 replicates, but its abundance gradually increased as the acetate production occurred later (Figure
487 S8). This correlation between acetate production and *Sporomusa* growth suggests that
488 *Sporomusa* is responsible for acetogenesis.
489 Apart from biotic bottle IV, no notable increase in acetate and propionate was observed after day
490 10, indicating that lactate fermentation and acetogenesis were much faster processes compared to
491 reductive dechlorination, and were primarily active during the early stages of 2,3-DCA
492 dechlorination (Figure S6). This is further supported by the amplicon sequencing results, which
493 revealed a continuous and significant decline of *Clostridium sensu stricto 7* and *Sporomusa* as
494 the experiment progressed. Beyond day 10, fermentation reactions were much slower owing to

495 lack of readily fermentable substrates. Once amended lactate and ethanol were depleted, the
496 abundance of dominant fermenting bacteria decreased, while *Dehalobacter* became the most
497 abundant bacterial genus (Figures 1e and S7a). Principal component analysis (PCA) of bacterial
498 community composition (detailed in Figure S10) reveals a temporal and reproducible succession
499 under chlorinated aniline stress, with biotic replicates (especially I, II, and III) converging along
500 a shared trajectory. Major community shifts on day 12 (marking the end of fermentation from
501 added donors) and day 50 (the transition between 2,3-DCA and 2-CA dechlorination) observed
502 in the PCA plot (Figure S10) support the proposed temporal dynamics of microbiological
503 processes (Figure 4) and align with VFA and dechlorination profiles.
504 A variety of fermenting bacteria are involved in interspecies electron transfer within the
505 microbial consortium. They converted fatty acids and alcohols, which *Dehalobacter* cannot
506 utilize for energy and cell synthesis, into hydrogen, formate, and acetate, all of which supported
507 dehalorespiration and growth by *Dehalobacter*. Previous studies have reported *Dehalobacter*
508 relies on hydrogen or formate as the electron donors for anaerobic respiration[50–52] and acetate as
509 a carbon source.[53] In this work, acetate uptake into biomass by *Dehalobacter*, estimated from the
510 overall energetic equation (Section S9), was small (< 0.1mM) and not observable amidst the high
511 acetate levels.

512 6.4.2 Syntrophic propionate oxidation to provide hydrogen and acetate for 513 *Dehalobacter*

514 During 2,3-DCA dechlorination to monochloroanilines, concentrations of both acetate and
515 propionate, the primary products from fermentation, were steady in the bottles. However,
516 following the depletion of 2,3-DCA and initiation of dechlorination of 2-CA to aniline,
517 propionate levels began to decrease (days 50 – 95), while acetate concentrations exhibited
518 minimal decline (Figure 1b). A moderate amount of methane was also produced over the same

519 period, following a phase of negligible methanogenesis throughout 2,3-DCA dechlorination
520 (Figure 1d). This late-stage methanogenesis can be attributed to the decrease in propionate
521 concentrations (biotic bottles I, II, and IV), with a recovery of 78 (± 11) % (n=3), calculated as
522 the electron equivalent ratio of the methane production to the reduction in propionate. Moreover,
523 this late-stage methanogenesis was associated with a rise in the bacterial abundance of
524 *Pelotomaculum* (Figure 1e). These are syntrophic propionate-oxidizing bacteria that are
525 obligately co-cocultured with methanogens.[54,55] Thus experimental evidence indicates that
526 propionate was consumed by *Pelotomaculum* via syntrophic oxidation. Subsequently, the
527 products from syntrophic propionate oxidation, formate and hydrogen, were used by
528 hydrogenotrophic methanogens to form methane and by *Dehalobacter* for 2-CA dechlorination.
529 The syntrophic oxidation of propionate had an important role in this anaerobic dechlorinating
530 system. Lactate fermentation observed in the initial stage of the experiment produced propionate
531 and acetate, which was not a hydrogen-yielding process. In addition, propionate cannot be
532 directly utilized by *Dehalobacter* or methanogens and therefore built up (days 10 – 50). Thanks
533 to *Pelotomaculum*, propionate was metabolized into formate and hydrogen, thus enhancing the
534 electron transfer efficiency from the amended lactate to hydrogen gas and keeping the propionate
535 concentration low.
536 Additionally, our results clearly demonstrate that syntrophic propionate oxidation and associated
537 hydrogenotrophic methanogenesis did not commence until the depletion of 2,3-DCA (Figure 1).
538 This relatively late onset of syntrophic propionate oxidation may result from the toxicity of 2,3-
539 DCA on *Pelotomaculum* or methanogens. Syntrophic propionate oxidation is energetically
540 unfavourable unless coupled with effective hydrogen-consuming processes (e.g., dechlorination
541 and methanogenesis) to maintain low hydrogen patrial pressures.[47] During 2,3-DCA

542 dechlorination, *Dehalobacter* likely outcompeted methanogens for hydrogen, as shown by the
543 consistent and reproducible dechlorination profiles, while methane production remained
544 minimal. However, the hydrogen demand for dechlorination, as previously discussed, was too
545 low to trigger the syntrophic propionate oxidation.

546 6.4.3 Acetate accumulation and potential inhibition of chloroanilines on 547 acetoclastic methanogens

548 The accumulation of acetate in the dechlorinating cultures was unexpected, but also observed in
549 our companion study[25]. Rather than methane, most of electrons from added lactate and ethanol
550 ended up in the form of acetate (Figure S8). The acetate accumulation suggests a lack of
551 effective acetate consumer in the community, which is further confirmed by the 16S rRNA
552 sequencing results (Figure S9). All identified methanogens, such as *Methanobacterium*, which
553 dominated the Archaea community with a relative abundance greater than 97%, and
554 *Methanoregula*, are hydrogenotrophic methanogens that produce methane exclusively from
555 hydrogen and CO_2 and not from acetate.[56,57] Thus, acetate accumulation was due to the absence
556 of acetoclastic methanogens. The absence of acetoclastic methanogens suggests they were
557 eliminated by elevated concentrations of chlorinated anilines, and effectively diluted out of the
558 culture after successive transfers. Previous studies have reported that chlorinated compounds and
559 amino-substituted aromatics can inhibit conversion of acetate to methane.[58,59] Similar acetate
560 accumulation under stress conditions was reported in tetrachloroethene-dechlorinating
561 microcosms exposed to high salinity, where upstream fermentation (acidogenesis and
562 hydrogenesis) remained active, but downstream consumers of fermentation products were
563 inhibited.[60] Excessive acetate not only led to a low electron transfer efficiency from the amended
564 electron donors to hydrogen gas but may also exhaust the buffering capacity of the mineral
565 medium, leading to low pH conditions that could harm the microbial system. Thus, for

566 dechlorinating microbial systems lacking the acetoclastic methanogens, regular culture transfer
567 can be a preventive measure against the excessive acetate. Moreover, acetate accumulation can
568 serve as a potential indicator of methanogenesis inhibition in the groundwater.

569 7 Environmental Implications

570 This study presents the stoichiometric reductive dechlorination of 2,3-DCA by *Dehalobacter*,
571 resulting primarily in aniline via 2-CA, but also in the low (<15%) yet persistent accumulation of
572 3-CA. This underscores the importance of monitoring transformation products during
573 dechlorination processes, which is analogous to the accumulation of vinyl chloride during
574 dichloroelimination of 1,2-diochloroethane to ethene.[61] Thanks to a unique high-frequency
575 sampling regime, we estimated kinetic parameters and growth yields that are valuable for
576 modeling the fate and transport of chloroanilines in groundwater and to quantify *in situ*
577 dechlorination. The syntrophic interactions between *Dehalobacter* and its microbial community
578 can be used as one line of evidence to identify natural attenuation of chlorinated anilines at
579 contaminated sites. Co-contaminants of chloroanilines at the site, primarily chlorobenzenes and
580 chloronitrobenzenes, likely exert selective pressure by favoring organohalide-respiring bacteria
581 such as *Dehalobacter*. *Dehalobacter* with broader dechlorination capabilities may have been
582 enriched through dechlorination of chlorobenzenes and chloroanilines that are also formed via
583 nitro-group reduction of chloronitrobenzenes, as observed in our companion study[25] using
584 cultures derived from the same site. In addition, the achievement of complete dechlorination at a
585 high substrate level (40 mg/L) with a low inoculum (3% v/v) holds promise for the application of
586 biostimulation (with electron donors) and bioaugmentation strategies to address chloroaniline
587 contamination. This study also explored interspecies electron transfer as a function of amended
588 donors over time, deciphering some of the dynamics of successive microbial processes, including

the issue of acetate accumulation, offering insights into establishing and maintaining a stable anaerobic dechlorinating system in culture or *in situ*. Although hydrogen was not directly quantified in this work, it is presumed to be the electron donor based on the observed fermentation pathways, electron balance, and the established physiology of *Dehalobacter*. While this work prioritized a mixed, field-derived consortium to reflect the site conditions, future studies should directly measure hydrogen and use it as the sole electron donor to confirm its role. Our ongoing work involves metagenomics and compound-specific isotope analysis to elucidate the reaction pathways of chlorine removal and determine isotope enrichment factors for field-based assessment of *in situ* dechlorination of chloroanilines.

8 ASSOCIATED CONTENT

The supporting information is available free of charge. Supplementary descriptions of subculture establishment, analytical methods, and data analysis, along with the relevant figures and tables discussed in the paper (PDF). Original data provided in spreadsheet format (.xlsx).

9 ACKNOWLEDGMENTS

This research was supported by the Natural Sciences and Engineering Research Council of Canada (NSERC) Discovery (RGPIN-2015-06460), Alliance (ALLRP 575243-22), and Canada Research Chair (950-230892) grants to E. Passeport, and a Mitacs (IT29192) grant to both E. Passeport and E. Edwards. The authors declare no conflicts of interest. This publication is in accordance with the Brazilian biodiversity law n.º 13.123, from May 20th, 2015. This is non-profit research and has no commercial intention between the parties. This is a collaboration project between the parties involved. Access Registration No. A3D9F11.

10 REFERENCES

(1) Vogt, P. F.; Gerulis, J. J. Amines, Aromatic. In *Ullmann's Encyclopedia of Industrial Chemistry*; Wiley-VCH, Ed.; Wiley, 2000. https://doi.org/10.1002/14356007.a02_037.

(2) Batista, S.; Silva, E.; Galhardo, S.; Viana, P.; José Cerejeira, M. Evaluation of Pesticide Contamination of Ground Water in Two Agricultural Areas of Portugal. *Int. J. Environ. Anal. Chem.* **2002**, *82* (8–9), 601–609. https://doi.org/10.1080/03067310290009488.

(3) Berrada, H.; Font, G.; Moltó, J. C. Application of Solid-Phase Microextraction for Determining Phenylurea Herbicides and Their Homologous Anilines from Vegetables. *J. Chromatogr. A* **2004**, *1042* (1–2), 9–14. https://doi.org/10.1016/j.chroma.2004.05.017.

(4) Oanh, N. T.; Duc, H. D. Anaerobic Degradation of Propanil in Soil and Sediment Using Mixed Bacterial Culture. *Curr. Microbiol.* **2021**, *78* (4), 1499–1508. https://doi.org/10.1007/s00284-021-02419-7.

(5) Ibrahim, M. A.; Zulkifli, S. Z.; Azmai, M. N. A.; Mohamat-Yusuff, F.; Ismail, A. Embryonic Toxicity of 3,4-Dichloroaniline (3,4-DCA) on Javanese Medaka (Oryzias Javanicus Bleeker, 1854). *Toxicol. Rep.* **2020**, *7*, 1039–1045. https://doi.org/10.1016/j.toxrep.2020.08.011.

(6) Philippe, C.; Hautekiet, P.; Grégoir, A. F.; Thoré, E. S. J.; Brendonck, L.; De Boeck, G.; Pinceel, T. Interactive Effects of 3,4-DCA and Temperature on the Annual Killifish Nothobranchius Furzeri. *Aquat. Toxicol.* **2019**, *212*, 146–153. https://doi.org/10.1016/j.aquatox.2019.05.009.

(7) Rodrigues, A. D.; dos Santos Montanholi, A.; Shimabukuro, A. A.; Yonekawa, M. K. A.; Cassemiro, N. S.; Silva, D. B.; Marchetti, C. R.; Weirich, C. E.; Beatriz, A.; Zanoelo, F. F.; Marques, M. R.; Giannesi, G. C.; das Neves, S. C.; Oliveira, R. J.; Ruller, R.; de Lima, D. P.; dos Anjos dos Santos, E. N-Acetylation of Toxic Aromatic Amines by Fungi: Strain Screening, Cytotoxicity and Genotoxicity Evaluation, and Application in Bioremediation of 3,4-Dichloroaniline. *J. Hazard. Mater.* **2023**, *441*, 129887. https://doi.org/10.1016/j.jhazmat.2022.129887.

(8) Klečka, G. M.; Carpenter, C. L.; Gonsior, S. J. Biological Transformations of 1,2-Dichloroethane in Subsurface Soils and Groundwater. *J. Contam. Hydrol.* **1998**, *34* (1–2), 139–154. https://doi.org/10.1016/S0169-7722(98)00096-5.

(9) Major, D. W.; McMaster, M. L.; Cox, E. E.; Edwards, E. A.; Dworatzek, S. M.; Hendrickson, E. R.; Starr, M. G.; Payne, J. A.; Buonamici, L. W. Field Demonstration of Successful Bioaugmentation To Achieve Dechlorination of Tetrachloroethene To Ethene. *Environ. Sci. Technol.* **2002**, *36* (23), 5106–5116. https://doi.org/10.1021/es0255711.

(10) Gieg, L. M.; Suflita, J. M. Detection of Anaerobic Metabolites of Saturated and Aromatic Hydrocarbons in Petroleum-Contaminated Aquifers. *Environ. Sci. Technol.* **2002**, *36* (17), 3755–3762. https://doi.org/10.1021/es0205333.

(11) Xu, G.; Zhao, S.; Chen, C.; Zhang, N.; He, J. Alleviating Chlorinated Alkane Inhibition on *Dehalococcoides* to Achieve Detoxification of Chlorinated Aliphatic Cocontaminants. *Environ. Sci. Technol.* **2023**, *57* (40), 15112–15122. https://doi.org/10.1021/acs.est.3c04535.

(12) Blázquez-Pallí, N.; Torrentó, C.; Marco-Urrea, E.; Garriga, D.; González, M.; Bosch, M. Pilot Tests for the Optimization of the Bioremediation Strategy of a Multi-Layered Aquifer

at a Multi-Focus Site Impacted with Chlorinated Ethenes. *Sci. Total Environ.* **2024**, *935*, 173093. https://doi.org/10.1016/j.scitotenv.2024.173093.

(13) Struijs, J.; Rogers, J. E. Reductive Dehalogenation of Dichloroanilines by Anaerobic Microorganisms in Fresh and Dichlorophenol-Acclimated Pond Sediment. *Appl. Environ. Microbiol.* **1989**, *55* (10), 2527–2531. https://doi.org/10.1128/aem.55.10.2527-2531.1989.

(14) Kuhn, E. P.; Suflita, J. M. Sequential Reductive Dehalogenation of Chloroanilines by Microorganisms from a Methanogenic Aquifer. *Environ. Sci. Technol.* **1989**, *23* (7), 848–852. https://doi.org/10.1021/es00065a014.

(15) Susarla, S.; Yonezawa, Y.; Masunaga, S. Reductive Transformations of Halogenated Aromatics in Anaerobic Estuarine Sediment: Kinetics, Products and Pathways. *Water Res.* **1998**, *32* (3), 639–648. https://doi.org/10.1016/S0043-1354(97)00265-0.

(16) Duc, H. D.; Oanh, N. T. Anaerobic Degradation of Chloroanilines by Geobacter Sp. KT5. *Curr. Microbiol.* **2019**, *76* (2), 248–257. https://doi.org/10.1007/s00284-018-1617-7.

(17) Cooper, M.; Wagner, A.; Wondrousch, D.; Sonntag, F.; Sonnabend, A.; Brehm, M.; Schüürmann, G.; Adrian, L. Anaerobic Microbial Transformation of Halogenated Aromatics and Fate Prediction Using Electron Density Modeling. *Environ. Sci. Technol.* **2015**, *49* (10), 6018–6028. https://doi.org/10.1021/acs.est.5b00303.

(18) Zhang, S.; Wondrousch, D.; Cooper, M.; Zinder, S. H.; Schüürmann, G.; Adrian, L. Anaerobic Dehalogenation of Chloroanilines by *Dehalococcoides Mccartyi* Strain CBDB1 and *Dehalobacter* Strain 14DCB1 via Different Pathways as Related to Molecular Electronic Structure. *Environ. Sci. Technol.* **2017**, *51* (7), 3714–3724. https://doi.org/10.1021/acs.est.6b05730.

(19) Suzana de Paula Queiroz Kraus. Aerobic and Anaerobic Biotransformation of Chloroanilines, Chlorobenzenes, and Dichlonitrobenzenes at a Complex Industrial Site in Brazil and Analysis of Associated Microbial Communities. Master Thesis, University of Toronto, 2018. http://hdl.handle.net/1807/91484.

(20) Barreto, P.; Lemes, M.; Jimenez, J.; Mack, E. E.; Henderson, J.; Freedman, D. L. Evaluation of Strategies to Remediate Mixed Wastes at an Industrial Site in Brazil. *Groundw. Monit. Remediat.* **2023**, *43* (3), 93–107. https://doi.org/10.1111/gwmr.12607.

(21) Melo, N.; Araújo, S. P.; De Paula Queiroz Kraus, S.; Lomheim, L.; Quintero, P. B.; Mack, E. E.; Edwards, E. A.; Spain, J.; Gavazza, S. Strategies for Bioremediation of Soil from an Industrial Site Exposed to Chlorinated and Nitroaromatic Compounds. *Groundw. Monit. Remediat.* **2023**, *43* (3), 108–120. https://doi.org/10.1111/gwmr.12596.

(22) Nelson, J. L.; Jiang, J.; Zinder, S. H. Dehalogenation of Chlorobenzenes, Dichlorotoluenes, and Tetrachloroethene by Three *Dehalobacter* Spp. *Environ. Sci. Technol.* **2014**, *48* (7), 3776–3782. https://doi.org/10.1021/es4044769.

(23) Bulka, O.; Webb, J.; Dworatzek, S.; Mahadevan, R.; Edwards, E. A. A Multifunctional *Dehalobacter* ? Tandem Chloroform and Dichloromethane Degradation in a Mixed Microbial Culture. *Environ. Sci. Technol.* **2023**, *57* (48), 19912–19920. https://doi.org/10.1021/acs.est.3c06686.

(24) Justicia-Leon, S. D.; Higgins, S.; Mack, E. E.; Griffiths, D. R.; Tang, S.; Edwards, E. A.; Löffler, F. E. Bioaugmentation with Distinct *Dehalobacter* Strains Achieves Chloroform Detoxification in Microcosms. *Environ. Sci. Technol.* **2014**, *48* (3), 1851–1858. https://doi.org/10.1021/es403582f.

(25) Sofia P. Araújo; Line Lomheim; Suzana P. Q. Kraus; E. Erin Mack; Jim C. Spain; Sávia Gavazza; Elizabeth A. Edwards. Dehalobacter Dechlorinates Dichloroanilines and

Contributes to the Natural Attenuation of Dichloronitrobenzenes at a Complex Industrial Site. *https://www.biorxiv.org/content/10.1101/2025.02.13.638192v1* **2025**.

(26) Edwards, E. A.; Grbić-Galić, D. Complete Mineralization of Benzene by Aquifer Microorganisms under Strictly Anaerobic Conditions. *Appl. Environ. Microbiol.* **1992**, *58* (8), 2663–2666. https://doi.org/10.1128/aem.58.8.2663-2666.1992.

(27) Grostern, A.; Edwards, E. A. Growth of Dehalobacter and Dehalococcoides Spp. during Degradation of Chlorinated Ethanes. *Appl. Environ. Microbiol. 2006, 72, (1)*, 428–436.

(28) Amann, R. I.; Ludwig, W.; Schleifer, K. H. Phylogenetic Identification and in Situ Detection of Individual Microbial Cells without Cultivation. *Microbiol. Rev.* **1995**, *59* (1), 143–169. https://doi.org/10.1128/mr.59.1.143-169.1995.

(29) Toth, C. R. A.; Luo, F.; Bawa, N.; Webb, J.; Guo, S.; Dworatzek, S.; Edwards, E. A. Anaerobic Benzene Biodegradation Linked to the Growth of Highly Specific Bacterial Clades. *Environ. Sci. Technol.* **2021**, *55* (12), 7970–7980. https://doi.org/10.1021/acs.est.1c00508.

(30) Bolyen, E.; Rideout, J. R.; Dillon, M. R.; Bokulich, N. A.; Abnet, C. C.; Al-Ghalith, G. A.; Alexander, H.; Alm, E. J.; Arumugam, M.; Asnicar, F.; Bai, Y.; Bisanz, J. E.; Bittinger, K.; Brejnrod, A.; Brislawn, C. J.; Brown, C. T.; Callahan, B. J.; Caraballo-Rodríguez, A. M.; Chase, J.; Cope, E. K.; Da Silva, R.; Diener, C.; Dorrestein, P. C.; Douglas, G. M.; Durall, D. M.; Duvallet, C.; Edwardson, C. F.; Ernst, M.; Estaki, M.; Fouquier, J.; Gauglitz, J. M.; Gibbons, S. M.; Gibson, D. L.; Gonzalez, A.; Gorlick, K.; Guo, J.; Hillmann, B.; Holmes, S.; Holste, H.; Huttenhower, C.; Huttley, G. A.; Janssen, S.; Jarmusch, A. K.; Jiang, L.; Kaehler, B. D.; Kang, K. B.; Keefe, C. R.; Keim, P.; Kelley, S. T.; Knights, D.; Koester, I.; Kosciolek, T.; Kreps, J.; Langille, M. G. I.; Lee, J.; Ley, R.; Liu, Y.-X.; Loftfield, E.; Lozupone, C.; Maher, M.; Marotz, C.; Martin, B. D.; McDonald, D.; McIver, L. J.; Melnik, A. V.; Metcalf, J. L.; Morgan, S. C.; Morton, J. T.; Naimey, A. T.; Navas-Molina, J. A.; Nothias, L. F.; Orchanian, S. B.; Pearson, T.; Peoples, S. L.; Petras, D.; Preuss, M. L.; Pruesse, E.; Rasmussen, L. B.; Rivers, A.; Robeson, M. S.; Rosenthal, P.; Segata, N.; Shaffer, M.; Shiffer, A.; Sinha, R.; Song, S. J.; Spear, J. R.; Swafford, A. D.; Thompson, L. R.; Torres, P. J.; Trinh, P.; Tripathi, A.; Turnbaugh, P. J.; Ul-Hasan, S.; Van Der Hooft, J. J. J.; Vargas, F.; Vázquez-Baeza, Y.; Vogtmann, E.; Von Hippel, M.; Walters, W.; Wan, Y.; Wang, M.; Warren, J.; Weber, K. C.; Williamson, C. H. D.; Willis, A. D.; Xu, Z. Z.; Zaneveld, J. R.; Zhang, Y.; Zhu, Q.; Knight, R.; Caporaso, J. G. Reproducible, Interactive, Scalable and Extensible Microbiome Data Science Using QIIME 2. *Nat. Biotechnol.* **2019**, *37* (8), 852–857. https://doi.org/10.1038/s41587-019-0209-9.

(31) Callahan, B. J.; McMurdie, P. J.; Rosen, M. J.; Han, A. W.; Johnson, A. J. A.; Holmes, S. P. DADA2: High-Resolution Sample Inference from Illumina Amplicon Data. *Nat. Methods* **2016**, *13* (7), 581–583. https://doi.org/10.1038/nmeth.3869.

(32) Quast, C.; Pruesse, E.; Yilmaz, P.; Gerken, J.; Schweer, T.; Yarza, P.; Peplies, J.; Glöckner, F. O. The SILVA Ribosomal RNA Gene Database Project: Improved Data Processing and Web-Based Tools. *Nucleic Acids Res.* **2012**, *41* (D1), D590–D596. https://doi.org/10.1093/nar/gks1219.

(33) Monod, J. The Growth of Bacterial Cultures. *Ann. Rev. Microbiol* **1949**, 3, 371-394.

(34) Pirt, S. J. *Principles of Microbe and Cell Cultivation*; Blackwell Scientific, 1975.

(35) Susarla, S.; Masunaga, S.; Yonezawa, Y. Redox Potential as a Parameter To Predict the Reductive Dechlorination Pathway of Chloroanilines in Anaerobic Environments. *Microb. Ecol.* **1997**, *33* (3), 252–256. https://doi.org/10.1007/s002489900028.

(36) Rittmann, B. E.; McCarty, P. L. *Environmental Biotechnology: Principles and Applications*, 2001st ed.; McGraw-Hill Education, 2001.
(37) McCarty, P. L. Thermodynamic Electron Equivalents Model for Bacterial Yield Prediction: Modifications and Comparative Evaluations. *Biotechnol. Bioeng.* **2007**, *97* (2), 377–388. https://doi.org/10.1002/bit.21250.
(38) Madigan, M. T.; Martinko, J. M.; Bender, K. S.; Buckley, D. H.; Stahl, D. A.; Brock, T. *Brock Biology of Microorganisms*, 14th ed.; Pearson Education, 2014.
(39) Seeliger, S.; Janssen, P. H.; Schink, B. Energetics and Kinetics of Lactate Fermentation to Acetate and Propionate via Methylmalonyl-CoA or Acrylyl-CoA. *FEMS Microbiology Letters* **2002**, *211* (1), 65–70.
(40) Leaver, F. W.; Wood, H. G.; Stjernholm, R. THE FERMENTATION OF THREE CARBON SUBSTRATES BY *CLOSTRIDIUM PROPIONICUM* AND *PROPIONIBACTERIUM*. *J. Bacteriol.* **1955**, *70* (5), 521–530. https://doi.org/10.1128/jb.70.5.521-530.1955.
(41) Stams, A. J. M.; Dijkema, C.; Plugge, C. M.; Lens, P. Contribution of 13C-NMR Spectroscopy to the Elucidation of Pathways of Propionate Formation and Degradation in Methanogenic Environments. **1998,** 9, 463-473. https://doi.org/10.1023/A:1008342130938.
(42) Fennell, D. E.; Gossett, J. M. Modeling the Production of and Competition for Hydrogen in a Dechlorinating Culture. *Environ. Sci. Technol.* **1998**, *32* (16), 2450–2460. https://doi.org/10.1021/es980136l.
(43) Litti, Yu. V.; Kovalev, D. A.; Kovalev, A. A.; Merkel, A. Yu.; Vishnyakova, A. V.; Russkova, Yu. I.; Nozhevnikova, A. N. Auto-Selection of Microorganisms of Sewage Sludge Used as an Inoculum for Fermentative Hydrogen Production from Different Substrates. *Int. J. Hydrog. Energy* **2021**, *46* (58), 29834–29845. https://doi.org/10.1016/j.ijhydene.2021.06.174.
(44) Tang, T.; Chen, Y.; Liu, M.; Du, Y.; Tan, Y. Effect of pH on the Performance of Hydrogen Production by Dark Fermentation Coupled Denitrification. *Environ. Res.* **2022**, *208*, 112663. https://doi.org/10.1016/j.envres.2021.112663.
(45) Yang, G.; Wang, J. Changes in Microbial Community Structure during Dark Fermentative Hydrogen Production. *Int. J. Hydrog. Energy* **2019**, *44* (47), 25542–25550. https://doi.org/10.1016/j.ijhydene.2019.08.039.
(46) Falkow, S.; Rosenberg, E.; Schleifer, K.-H.; Stackebrandt, E. *The Prokaryotes: Vol. 4: Bacteria: Firmicutes, Cyanobacteria*; Springer Science & Business Media, 2006; Vol. 4.
(47) Schink, B. Energetics of Syntrophic Cooperation in Methanogenic Degradation. *Microbiol. Mol. Biol. Rev.* **1997**, *61* (2), 262–280. https://doi.org/10.1128/mmbr.61.2.262-280.1997.
(48) Schink, B. Anaerobic Digestion: Concepts, Limits and Perspectives. *Water Science and Technology* **2002**, *45* (10), 1–8.
(49) Schuchmann, K.; Müller, V. Energetics and Application of Heterotrophy in Acetogenic Bacteria. *Appl. Environ. Microbiol.* **2016**, *82* (14), 4056–4069. https://doi.org/10.1128/AEM.00882-16.
(50) Fincker, M.; Spormann, A. M. Biochemistry of Catabolic Reductive Dehalogenation. *Annu. Rev. Biochem.* **2017**, *86* (1), 357–386. https://doi.org/10.1146/annurev-biochem-061516-044829.
(51) Wang, S.; Qiu, L.; Liu, X.; Xu, G.; Siegert, M.; Lu, Q.; Juneau, P.; Yu, L.; Liang, D.; He, Z.; Qiu, R. Electron Transport Chains in Organohalide-Respiring Bacteria and

Bioremediation Implications. *Biotechnol. Adv.* **2018**, *36* (4), 1194–1206. https://doi.org/10.1016/j.biotechadv.2018.03.018.

(52) Sun, B.; Griffin, B. M.; Ayala-del-Río, H. L.; Hashsham, S. A.; Tiedje, J. M. Microbial Dehalorespiration with 1,1,1-Trichloroethane. *Science* **2002**, *298* (5595), 1023–1025. https://doi.org/10.1126/science.1074675.

(53) Holliger, C.; Hahn, D.; Harmsen, H.; Ludwig, W.; Schumacher, W.; Tindall, B.; Vazquez, F.; Weiss, N.; Zehnder, A. J. B. Dehalobacter Restrictus Gen. Nov. and Sp. Nov., a Strictly Anaerobic Bacterium That Reductively Dechlorinates Tetra- and Trichloroethene in an Anaerobic Respiration. *Arch. Microbiol.* **1998**, *169* (4), 313–321. https://doi.org/10.1007/s002030050577.

(54) Bok, F. A. M.; Harmsen, H. J. M.; Plugge, C. M.; de Vries, M. C.; Akkermans, A. D. L.; de Vos, W. M.; Stams, A. J. M. The First True Obligately Syntrophic Propionate-Oxidizing Bacterium, Pelotomaculum Schinkii Sp. Nov., Co-Cultured with Methanospirillum Hungatei, and Emended Description of the Genus Pelotomaculum. *Int. J. Syst. Evol. Microbiol.* **2005**, *55* (4), 1697–1703. https://doi.org/10.1099/ijs.0.02880-0.

(55) Imachi, H.; Sakai, S.; Ohashi, A.; Harada, H.; Hanada, S.; Kamagata, Y.; Sekiguchi, Y. Pelotomaculum Propionicicum Sp. Nov., an Anaerobic, Mesophilic, Obligately Syntrophic, Propionate-Oxidizing Bacterium. *Int. J. Syst. Evol. Microbiol.* **2007**, *57* (7), 1487–1492. https://doi.org/10.1099/ijs.0.64925-0.

(56) Bräuer, S. L.; Cadillo-Quiroz, H.; Ward, R. J.; Yavitt, J. B.; Zinder, S. H. Methanoregula Boonei Gen. Nov., Sp. Nov., an Acidiphilic Methanogen Isolated from an Acidic Peat Bog. *Int. J. Syst. Evol. Microbiol.* **2011**, *61* (1), 45–52. https://doi.org/10.1099/ijs.0.021782-0.

(57) Schonheit, P.; Moll, J.; Thauer, R. K. Nickel, Cobalt, and Molybdenum Requirement for Growth of Methanobacterium Thermoautotrophicum. *Arch. Microbiol.* **1979**, *123* (1), 105–107. https://doi.org/10.1007/BF00403508.

(58) Donlon, B. A.; Razo-Flores, E.; Field, J. A.; Lettinga, G. Toxicity of N-Substituted Aromatics to Acetoclastic Methanogenic Activity in Granular Sludge. *Appl. Environ. Microbiol.* **1995**, *61* (11), 3889–3893. https://doi.org/10.1128/aem.61.11.3889-3893.1995.

(59) Yang, J.; Speece, R. E. The Effects of Chloroform Toxicity on Methane Fermentation. *Water Res.* **1986**, *20* (10), 1273–1279. https://doi.org/10.1016/0043-1354(86)90158-2.

(60) Xu, G.; Zhao, X.; Zhao, S.; Rogers, M. J.; He, J. Salinity Determines Performance, Functional Populations, and Microbial Ecology in Consortia Attenuating Organohalide Pollutants. *ISME J.* **2023**, *17* (5), 660–670. https://doi.org/10.1038/s41396-023-01377-1.

(61) Yu, R.; Peethambaram, H. S.; Falta, R. W.; Verce, M. F.; Henderson, J. K.; Bagwell, C. E.; Brigmon, R. L.; Freedman, D. L. Kinetics of 1,2-Dichloroethane and 1,2-Dibromoethane Biodegradation in Anaerobic Enrichment Cultures. *Appl. Environ. Microbiol.* **2013**, *79* (4), 1359–1367. https://doi.org/10.1128/AEM.02163-12.